Available online at www.sciencedirect.com

ScienceDirect

journal homepage: http://www.elsevier.com/locate/acme

Original Research Article

Influence of ALD process parameters on the physical and chemical properties of the surface of vascular stents

Marcin Basiaga [a,*], *Witold Walke* [a], *Marcin Staszuk* [b], *Wojciech Kajzer* [a], *Anita Kajzer* [a], *Katarzyna Nowińska* [c]

[a] *Faculty of Biomedical Engineering, Silesian University of Technology, Zabrze, Poland*
[b] *Faculty of Mechanical Engineering, Silesian University of Technology, Gliwice, Poland*
[c] *Faculty of Mining and Geology, Silesian University of Technology, Gliwice, Poland*

ARTICLE INFO

Article history:
Received 28 February 2016
Accepted 3 August 2016
Available online

Keywords:
316LVM steel
TiO_2
ALD
Electrochemical properties
Mechanical properties

ABSTRACT

Studies of haemocompatibility of AISI 316LVM steel point to the need for nickel elimination from the surface and replacing it with other elements showing higher biotolerance. Such layers include titanium, carbon or silicon coatings. Therefore, the authors attempted to evaluate some selected physicochemical properties of TiO_2 layers, grown by atomic layer deposition (ALD) method, on the surface of 316LVM steel at variable process temperature. ALD temperature has a major role in the final quality of the surface layer grown with the use of such method, regardless of the type of the base. It was observed that the growth of temperature had an adverse influence on corrosive resistance in the artificial plasma environment and contributed to formation of a double (porous) layer showing decreased tightness. Further on, assessment of the coating adhesion to the base showed that too low process temperature $T = 100\ ^{\circ}C$ had an adverse effect on mechanical properties, resulting in substantially reduced critical force. On the other hand, the performed surface wettability tests showed no influence of ALD temperature in the obtained angle values.

© 2016 Politechnika Wrocławska. Published by Elsevier Sp. z o.o. All rights reserved.

1. Introduction

Comprehensive improvement of quality of AISI 316LVM steel, used to manufacture intravascular implants, should focus on modelling of the surface layer structure, also taking into account the medical sterilization process. A factor of crucial importance is haemocompatibility, directly influenced by mechanical and electrochemical properties as well as surface wettability associated with its topography and chemical structure. Generally, the questions of modification of AISI 316LVM steel surface have been described widely in the literature. Surface modification has made use of a variety of methods. Such procedures aimed on the one hand at preparation of the modified surfaces for subsequent processing of the surface and on the other to ensure the demanded

* *Corresponding author.*
E-mail address: marcin.basiaga@polsl.pl (M. Basiaga).
http://dx.doi.org/10.1016/j.acme.2016.08.001
1644-9665/© 2016 Politechnika Wrocławska. Published by Elsevier Sp. z o.o. All rights reserved.

cell adhesion, proliferation and migration. For metal implants made of AISI 316LVM steel, blood in a corrosive environment. Blood concentrations of sodium bicarbonate ($NaHCO_3$), monobasic and dibasic acidic sodium phosphate (NaH_2PO_4 and $NaHPO_4$), proteins and erythrocyte haemoglobin ensure constant appropriate pH value, required for homeostasis, while on the other hand, it triggers the corrosive process. In order to prevent such an adverse phenomenon, surface layers of improved corrosive resistance are more commonly used. Studies of haemocompatibility of AISI 316LVM steel point to the need for nickel elimination from the surface and replacing it with other elements showing higher biotolerance. Such layers include carbon or silicon coatings. Ratner et al. [1] proposed in his studies a silicon carbide coat with amorphic structure, showing high athrombogenicity and susceptibility to deformation. Further on, the absence of cytotoxic response and no mutagenic effect upon the blood cells were shown by Fedel [2]. Also, attention is focused more often on titanium in the most thermodynamically stable form which is the semiconductive in structure (nonstoichiometric) – TiO_2. Such oxide is distinguished by a wide passive range, reaching even the value of several volts [3,4]. It is possible to form such layers ensuring good adhesion the base, abrasive resistance and protecting steel against the corrosive processes. Krishna et al. [5] prepared TiO_2 coatings on stainless steel, and they found that the stainless steel showed improved corrosion resistance with TiO_2 coatings. Shen et al. [6] reported the corrosion protection of 316 L stainless steel by uniform TiO_2 nanoparticulate coatings prepared by sol–gel method. They found that the TiO_2 coatings exhibited very good corrosion resistance by acting as a protective barrier on the steel surface. Thanks to good optical properties of TiO_2, the grown oxide layers show different colouration, depending in the layer thickness [4,7] which may prove helpful for identification of particular devices along a size series. In case of vascular stents, one of the crucial aspects is ensuring stability of geometrical features throughout their length. In such context, the most appropriate surface modification is coating with the use of atomic layer deposition [8–10]. In deposition of atomic layers the area of solid phase formation is restricted to a monomolecular adsorption layer. This has been achieved through alternating precursor pulses into the reaction chamber. Moreover, following each precursor pulse, the reaction side-products and unadsorbed particles are removed from the reaction chamber with the use of an inert gas. As a result, the gas phase precursors do not contact with each other, except for the adsorption layer. The earlier studies by the authors [11] showed a favourable effect of TiO_2 coat, formed by ALD, on the physicochemical properties of 316LVM steel. It was observed that the best scheme of physicochemical properties was achieved with films grown during 500 cycles of the process – Fig. 1. Apart from the number of cycles, an important parameter determining the coat properties, is the process temperature. Therefore, the authors attempted to evaluate some selected physicochemical properties of TiO_2 layers, grown by ALD method, on the surface of 316LVM steel at variable process temperature.

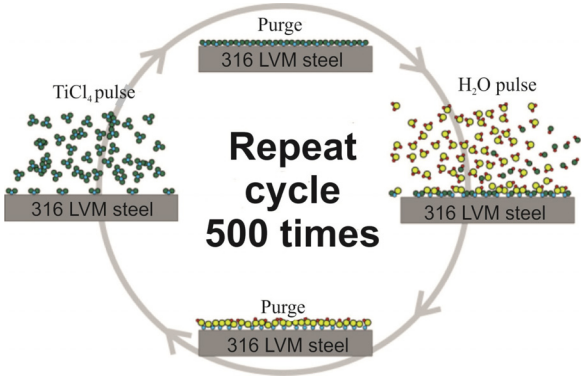

Fig. 1 – Scheme of ALD technique.

2. Materials and methods

2.1. *Preparation of samples*

Selected for the test was Cr–Ni–Mo (AISI 316LVM) steel in the form of discs with diameter $d = 14$ mm and thickness $g = 2$ mm. Before surface modification all the samples were electrochemically polished in the phosphate sulphate acid bath until the surface roughness of Ra < 0.12, recommended for circulatory devices, was achieved. The samples were then passivated in 40% HNO_3. Those are the basic stages of surface preparation of steel used to manufacture implants with miniaturized geometrical features. The prepared samples were coated with a TiO_2 layer with the use of atomic layer deposition (ALD). The TiO_2 films investigated in this study were grown from $TiCl_4$ and H_2O in a low-pressure ALD reactor [12,13]. The deposition process consisted of repeated ALD cycles. Each cycle included a $TiCl_4$ pulse, the purge time, H_2O pulse and another purge time. The process comprised a constant number of 500 cycles at the temperatures of: 100 °C, 200 °C, 300 °C and 400 °C – Fig. 1.

For evaluation of the effect of TiO_2 film deposition temperatures on the physicochemical properties of the assumed surface modification, the authors proposed the electrochemical, morphological, surface wettability and mechanical tests.

2.2. *Electrochemical properties*

2.2.1. *Potentiodynamic test*

The first to be carried out were pitting resistance tests with the potentiodynamic method, recording the polarization curves, as recommended by ASTM standard [14]. The test stand comprised VoltaLab PGP201 potentiostat, the reference electrode (type KP-113 saturated calomel electrode SCE), the supporting electrode (type PtP-201 platinum electrode), the anode (test sample) and a PC with VoltaMaster 4 software. The corrosive tests started with establishment of the open circuit potential E_{OCP} at electroless conditions. The polarization curves were recorded starting with the initial potential value, $E_{init} = E_{OCP} - 100$ mV. The potential changed along the anode direction at the rate of 0.16 mV/s. Once the anodic current density reached the value of 1 mA/cm^2, the polarization direction was changed. On the basis of the curves the corrosive potential E_{corr}, the breakthrough potential E_b, the

repassivation potential E_{cp}, and the transpassivation potential E_{tr}, were determined along with the value of the polarization resistance R_p, calculated with the use of Stern method. The resistance value was calculated from Eq. (1). Evaluation of the pitting resistance was carried out in the environment of artificial plasma with the chemical composition recommended by the standard [15] at the temperature $T = 37 \pm 1\,^{\circ}C$, and pH = 7.0 ± 0.2:

$$\Delta E/\Delta i_p = b_k b_a/2,3 i_{corr}(b_a + b_k) \quad [\Omega\,cm^2] \tag{1}$$

2.2.2. EIS test

The impedance measurements were taken with the use of Auto Lab PGSTAT 302N system provided with FRA2 (Frequency Response Analyser) module, in the artificial plasma at the temperature $T = 37 \pm 1\,^{\circ}C$, and pH = 7.0 ± 0.2. The tests made use of a three electrode system: a saturated calomel electrode SCE as a reference electrode, a supporting electrode (platinum rod) and working electrode – the tested sample – Fig. 2. Such measurement system made it possible to perform tests within 10^4–10^{-3} Hz frequency range. The sinusoid voltage amplitude of the activating signal was 10 mV. During the test, impedance spectra of the system were determined and the measurement data confronted against the equivalent system. The impedance spectra of the evaluated system were presented as Nyquist plots for different frequencies and as Bode diagrams. Selection of such method made it possible to characterize impedance of the phase boundary: AISI 316LVM steel – TiO_2 film – artificial plasma, through approximation of the impedance data with an electric equivalent circuit model.

2.2.3. Ions infiltration study

In order to assess coating density of the surface layer and also the amount of ions infiltrating from steel substrate to artificial plasma solution, metallic ions permeability tests were performed. The amount of ions Fe, Cr, Ni, Mo and Ti that infiltrated to the solution was designated. Each sample was placed for 28 days in 100 ml of artificial plasma at the temperature of $T = 37 \pm 1\,^{\circ}C$. Metallic ions concentrations were measured with spectrometer JY 2000, by Yobin–Yvon, applying ICP-AES method. The source of induction was plasma torch coupled with generator of frequency 40.68 MHz. When making analytical curve, diluted analytical materials by Merck were applied [4].

2.3. Surface morphology

2.3.1. AFM test

Taking into account a remarkable effect upon the early and late response of the stented vessels, the surface morphology of the prepared samples was evaluated with the use of AFM microscope, a non-contact mode selected. The scanned area was 10 μm × 10 μm at the resolution of 256 × 256.

2.3.2. SEM analysis

Additionally observation was carried out with the use of scanning electron microscope SUPRA 35 by ZEISS with secondary electron (SE) detection, within the magnification range 1000–70,000×. Accelerating voltage was equal 5.00 kV.

2.4. Surface wettability

In order to determine the surface wettability of the selected samples, the wetting angle and surface free energy (SFE) were evaluated with the use of Owens–Wendt method. The wettability angle measurement were performed with two liquids: distilled water (θw) (by Poch S.A.) and diiodomethane (by Merck). Measurements with a drop of liquid and diiodomethane spread over the sample surface were carried out at room temperature ($T = 23\,^{\circ}C$) at the test stand incorporating SURFTENS UNIVERSAL goniometer by OEG and a PC with Surftens 4.5 software to assess the recorded drop image. 5 drops of distilled water and diiodomethane each, 1.5 μl volume each, were placed on the surface of each of the samples. The measurement started 20 s after the drops were dripped. Duration of a single measurement was 60 s at the sampling frequency 1 Hz. The mean values of the wetting angle θ_{av} and the surface free energy γ^S were illustrated graphically. The values of surface free energy (SFE) assumed for the calculations, including their polar and dispersion components are given in Table 1.

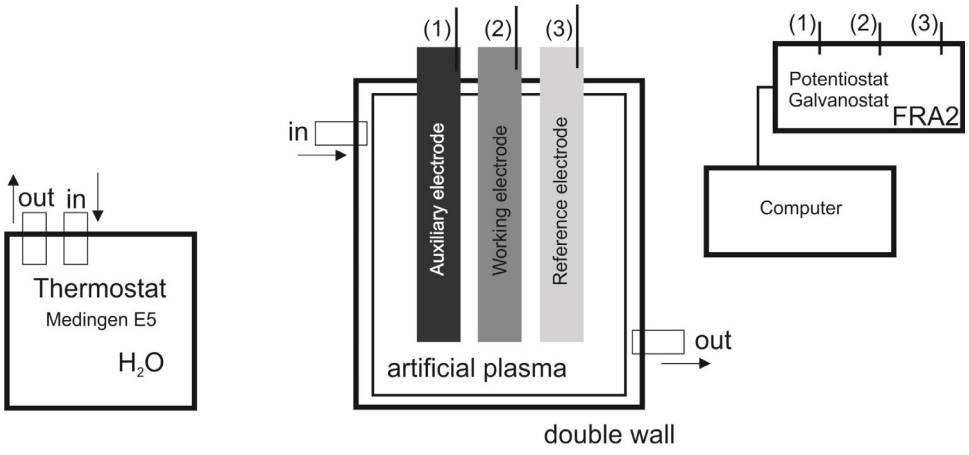

Fig. 2 – Scheme of the corrosion test.

Table 1 – The values of SEP and their individual components for measurement liquids.

Type of liquid	Polar component γ_s^p, mJ/m^2	Dispersion component γ_s^d, mJ/m^2
Distilled water	51.0	21.8
Diiodomethane	6.7	44.1

2.5. *Mechanical properties*

2.5.1. *Scratch test*

Adhesion of TiO_2 film to 316LVM steel base was evaluated with the use of a scratch test [16]. During the test a scratch was made with the use of Rockwell diamond cone with gradual growth of the indenter normal load. The critical force, a measure of adhesion, is the minimum normal force causing the loss of adhesion of the coat to the base. Evaluation of the critical force L_c based on the record of changes in acoustic emission, friction force and friction coefficient as well as microscopic inspection with a light microscope, integrated with the platform. Tests were performed at the loading force growing from $F_c = 0.03$ to 30 N and at the following working parameters: loading rate $v_s = 100$ N/min; table travel rate $v_t = 10$ mm/min, scratch length $l = 3$ mm.

2.5.2. *Nanohardness test*

The hardness assays with Oliver & Pharr method made use of Berkovich indenter [17]. The growth rate of the loading and unloading forces was 0.10 mN/min. The film nanohardness was measured on Nano-Combi-Tester open platform by CSM Instruments. The loading force value was 0.05 mN.

3. Results

3.1. *Electrochemical properties*

3.1.1. *Potentiodynamic test*

Results of potentiodynamic tests carried out to evaluate the pitting resistance are presented in Table 2 and Figs. 3 and 4. Earlier results obtained by the authors for electrochemically polished and chemically passivated 316LVM steel made it possible to define the corrosive potential E_{corr}, the value of which ranged between −166 mV and −256 mV. It was also observed that the value of transpassivation potential was E_{tr} = +1198 mV, while the polarization resistance $R_p = 211$ kΩ cm^2. Similar values of the breakthrough potential and the polarization resistance were obtained by the authors [18,19] in investigations of implants manufactured of CrNiMo steel,

Table 2 – Results of potentiodynamic tests – mean values.

Temperature of the ALD process	E_{corr}, mV	STD	E_b, mV	STD	E_{cp}, mV	STD	E_{tr}, mV	STD	R_p, kΩ cm^2	STD
100 °C	−174	±20	+1408	±15	+1143	±66	–	–	252	±57
200 °C	−214	±60	+1584	±48	+1389	±5	–	–	415	±83
300 °C	−138	±3	+1608	±16	+1363	±12	–	–	276	±20
400 °C	−177	±18	+1168	±317	+408	±647	–	–	204	±34

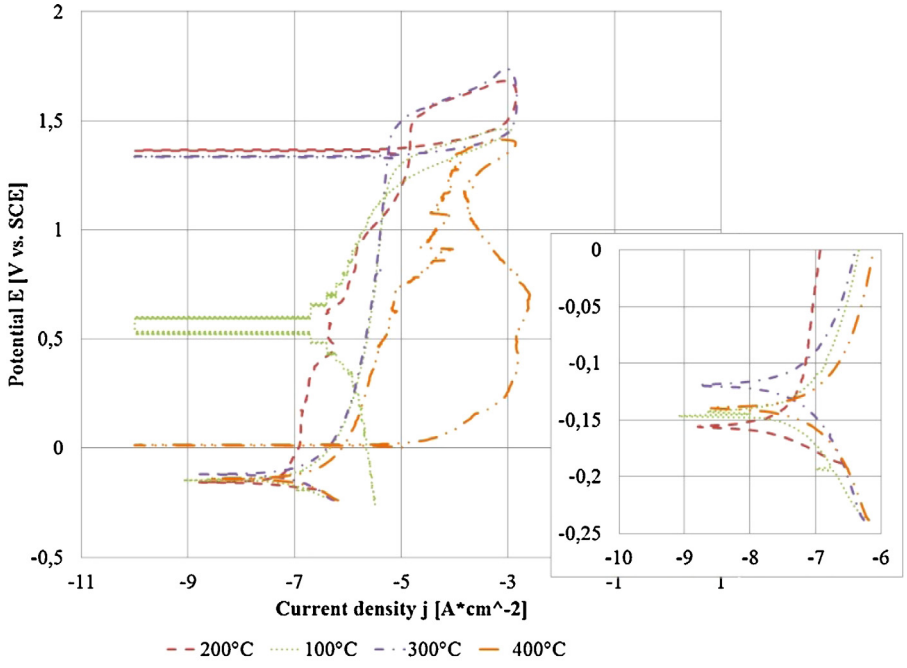

Fig. 3 – Polarization curves regarding AISI 316LVM after TiO_2 ALD surface modification. Area of corrosion potentials.

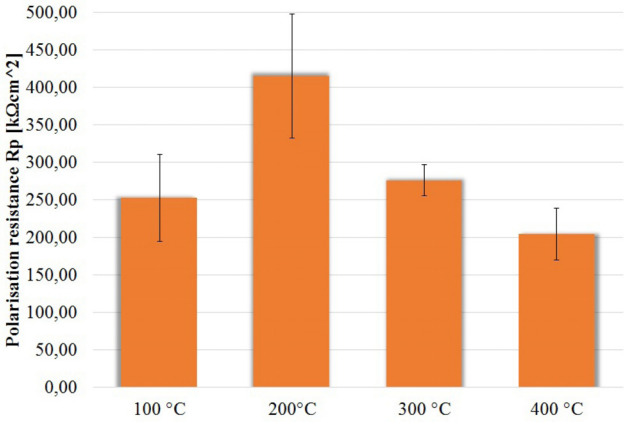

Fig. 4 – Comparison of polarization resistance R_p after surface modification.

after electrochemical polishing. However, in samples with the TiO_2 film deposited by ALD method, the breakthrough potential E_b and the repassivation potential E_{cp}, proving initiation and development of pitting corrosion, were noted regardless of the process temperature. The mean values of the breakthrough potential for most of the evaluates variants were higher than the transpassivation potentials E_{tr}, established for the initial state [11] and ranged between E_b = +1168 mV and E_b = +1608 mV. Moreover, the recorded values of repassivation potential E_{cp} for samples after ALD at temperatures T = 200 °C and T = 300 °C, were higher than the determined breakthrough potentials for layers grown at temperatures T = 100 °C and T = 400 °C – Table 2. The results confirm those reported by Marin and Shan [20–22], who also observed the effect of ALD on improved corrosive resistance of austenitic steel, as compared to the material at the initial state. In particular, they noted lowered current density and enlarged area of perfect passivation, as compared to samples with no oxide layer grown.

3.2. *EIS test*

The following stage of the study aimed at evaluation of the electrochemical properties though the impedance tests (EIS). The frequency measurements pointed to the amplitude-phase $Z''(Z')$ as well as amplitude $|Z(f)|$ and phase $\Theta(f)$ characteristics of the corrosive process, presented in Fig. 5. The recorded impedance points to differentiated kinetics of the corrosive processes taking place in the system AISI 316LVM steel – artificial plasma – Fig. 5. Structural optimization of a circuit reflecting the corrosive process in the evaluated system made use of a procedure based in Levenberg–Marquardt numerical algorithm of mean squared error minimization. It was proposed to apply two constant phase elements in the electric equivalent system, which improved the fitting quality of experimentally drawn curves, where R_s stands for the electrolyte resistance (artificial plasma), CPE_p – capacity of the extensive surface area of the material and R_p – the electrolyte resistance in this area of the material and R_{ct} and CPE_{dl} – standing for impedance and capacity of the double layer – Fig. 6.

A mathematical impedance model of the above system is also illustrated by Eq. (2):

$$Z = R_s + \frac{1}{(1/R_p) + Y_0(j\omega)^{n_1}} + \frac{1}{(1/R_{ct}) + Y_0(j\omega)^{n_2}} \quad (2)$$

Based on the equivalent schemes. Characteristic values have been defined to describe the corrosive resistance at different values if anode oxidation potential – Table 3.

3.3. *Ions infiltration*

The results of investigations of metallic ion infiltration, penetrating the artificial plasma after 28-day storage of AISI 316LVM steel samples, depending on the process temperature, are presented in Table 4. Assessment of chemical composition of the artificial plasma, where the samples were stored, allowed for establishment of Fe, Cr, Ni, Mo and Ti ions presence, regardless of temperature. Assuming that the quantity of degradation products infiltrating the artificial plasma is an important criterion indicative of the level of haemocompatibility of an evaluated material, it should be noted that the film deposition temperature, with the same number of cycles, effects the barrier properties. It was observed that the number of ions infiltrating the solution grows along with the increasing temperature. This is an adverse phenomenon which may result in allergic reaction and impair the implant healing. The most favourable properties protecting the alloy against the effect of a corrosive environment was achieved with the layers deposited at the temperatures of 100 °C and 200 °C.

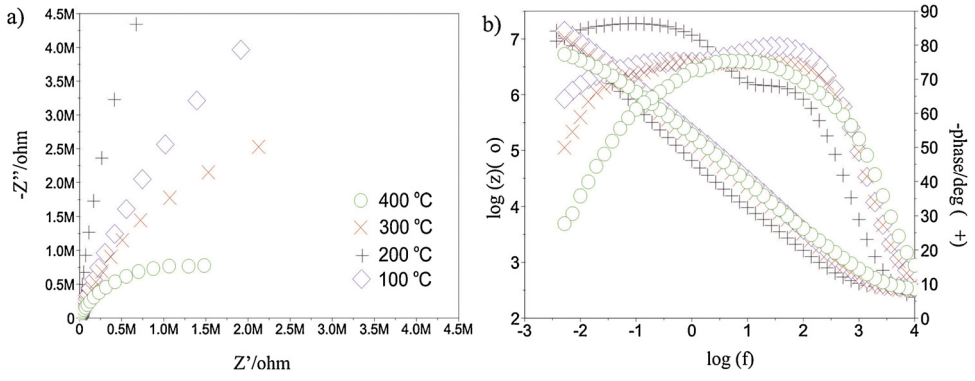

Fig. 5 – Examples of impedance spectra recorded for AISI 316LVM steel in the artificial plasma environment.

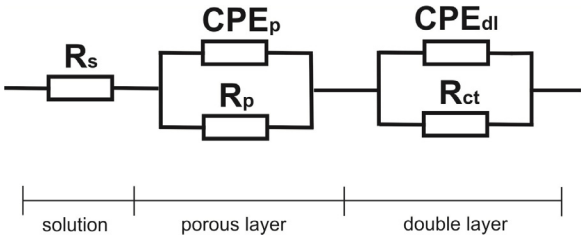

Fig. 6 – Electrical model of equivalent circuit for AISI 316LVM – TiO_2 layer – artificial plasma.

3.4. *Surface morphology*

Results of surface topography evaluation with the use of the atomic force microscope (AFM) and the scanning electron microscope (SEM) showed differences in the surface morphology (Figs. 7 and 8). The observed changes in morphology of the layers deposited at the temperatures of 200 °C and 300 °C resulted in elevated surface roughness, growing from Ra = 4 nm (T = 100 °C and 400 °C) up to Ra = 7 nm. In all the cases, the roughness values did not exceed Ra = 100 nm, recommended for such medical devices. Similar results were obtained by Aarik et al. [23] for increased number of deposition

Table 3 – Results of EIS tests.

Temperature of the ALD process	R_s, Ω cm^2	R_{pore}, kΩ cm^2	CPE_{pore}		R_{ct}, MΩ cm^2	CPE_{dl}		E_{OCP}, mV
			Y_0, Ω^{-1} cm^{-2} s^{-n}	n		Y_0, Ω^{-1} cm^{-2} s^{-n}	n	
100 °C	26	55	0.9716E−5	0,97	15.20	0.3749E−5	0.88	−288
200 °C	26	15	0.8268E−5	0,81	43.50	0.2002E−4	0.81	−268
300 °C	25	65	0.2328E−4	0,98	6.75	0.4322E−5	0.85	−227
400 °C	27	26	0.1626E−4	0,98	2.07	0.3923E−4	0.81	−280

Table 4 – Results of metallic ions infiltration.

Surface	Metallic ions infiltration tests, ppm (average value)									
	Fe	SD	Cr	SD	Ni	SD	Mo	SD	Ti	SD
100	0.099	±0.002	–	–	–	–	0.099	±0.001	0.105	±0.001
200	0.104	±0.001	–	–	–	±0.002	0.105	±0.002	0.112	±0.002
300	0.111	±0.001	0.022	±0,001	0.089	±0.001	0.110	±0.001	0.120	±0.001
400	0.121	±0.001	0.029	±0,001	0.095	±0.001	0.121	±0.001	0.134	±0.001

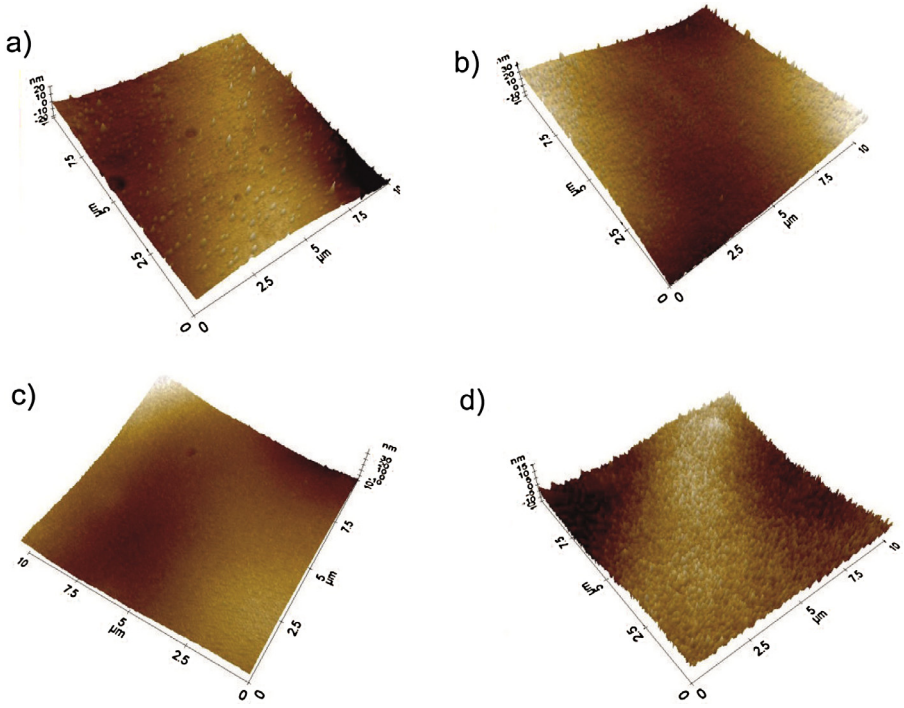

Fig. 7 – Surface morphology of samples with ALD deposited TiO_2 film at temperatures (AFM): (a) 100 °C, (b) 200 °C, (c) 300 °C, (d) 400 °C.

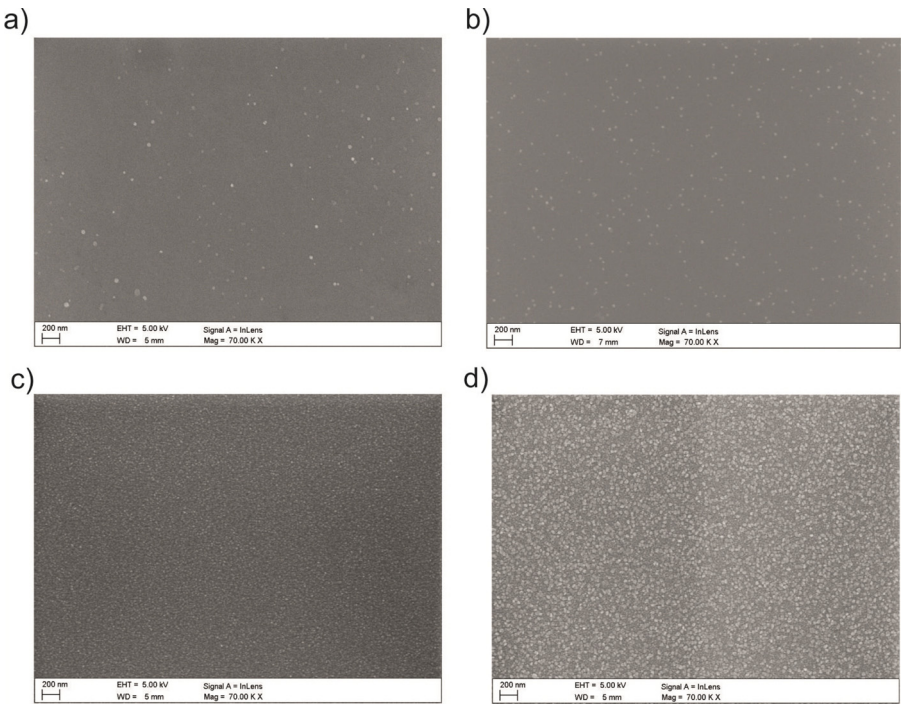

Fig. 8 – Surface morphology of samples with ALD deposited TiO_2 film at temperatures (SEM): (a) 100 °C, (b) 200 °C, (c) 300 °C, (d) 400 °C.

cycles (3000). On this basis it can be concluded that number of deposition cycles do not influence surface topography. The number of cycles suggested by the authors (500) caused reduction of the deposition time, allowing to keep similar parameters describing surface topography.

3.5. *Surface wettability*

The results of wettability and surface energy calculations and examples of drops dripped in the surface of samples with TiO_2 coat are presented in Figs. 9 and 10.

The obtained results pointed to the increased values of the wetting angle θ for the samples of AISI 316LVM with ALD deposited TiO_2 layer. The electrochemically polished and passivated samples are hydrophilic and show very low surface wettability [24]. Deposition of the TiO_2 film over the studied samples effected in the elevated wetting angle, regardless of the process temperature, resulting therefore in the hydrophobic surfaces – Fig. 9. No significant differences were observed in the values of the surface energy throughout the investigated sample surfaces. The study indicated that steel with the deposited TiO_2 layer showed higher wetting angle as

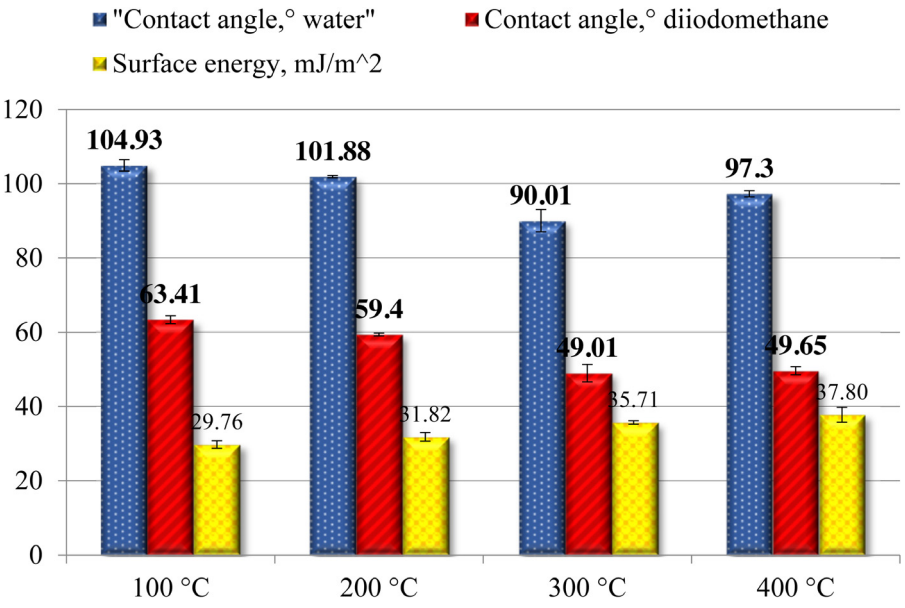

Fig. 9 – The surface energy calculated on the basis of the contact angle measurements – OW method.

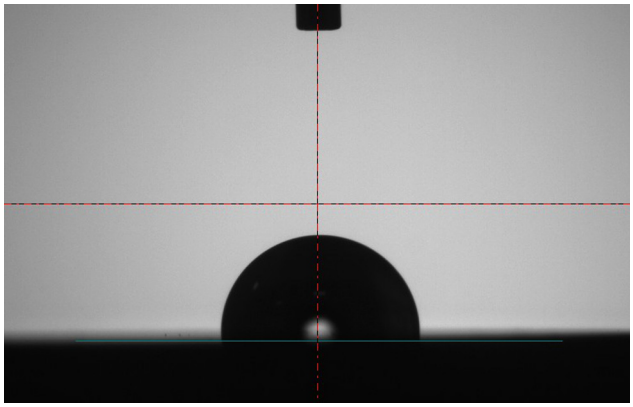

Fig. 10 – Sample measurement of wetting angle of TiO_2 film at temperature 200 °C (θ_{av} = 101.88°).

compared to the values obtained in surfaces after polishing and passivation. All the wetting angle values in samples with the TiO_2 layer were $\theta_{av} > 90°$ which proved the hydrophobic properties of the evaluated surfaces and appeared as a favourable phenomenon for the blood-contacting implants [25] contrary to investigations by the authors [26], who grew silicon films on steel samples with the use of sol–gel method, observing increased wettability in all variants of the investigated coatings, as compared to polished samples, which is an adverse feature in case of blood-contacting biomaterials.

Table 5 – Adhesion of TiO_2 layers to 316LVM steel.

Temperature of the ALD process	Failure of the layer	The value of registered indenter load Fn, mN	
		Average	Standard deviation
100	Delamination Lc_1	1070	±210
	Complete break Lc_2	5330	±540
200	Delamination Lc_1	3490	±225
	Complete break Lc_2	7220	±674
300	Delamination Lc_1	3860	±370
	Complete break Lc_2	8020	±542
400	Delamination Lc_1	380	±99
	Complete break Lc_2	3140	±1461

3.6. *Mechanical properties*

3.6.1. *Scratch test*

The obtained results pointed to the effect of TiO_2 deposition temperature on the critical force Lc, which is the measure of adhesion – Table 5. The best adhesion to 316LVM steel base was shown by samples with TiO_2 film deposited at the temperatures T = 200 °C and T = 300 °C. In such cases, the value of critical force causing the layer outward and inward delamination was respectively Lc_2 = 7220 mN (for T = 200 °C) and Lc_2 = 8020 mN (for T = 300 °C) – Fig. 11. Regardless of the sample type, no acoustic signal was recorded which proved

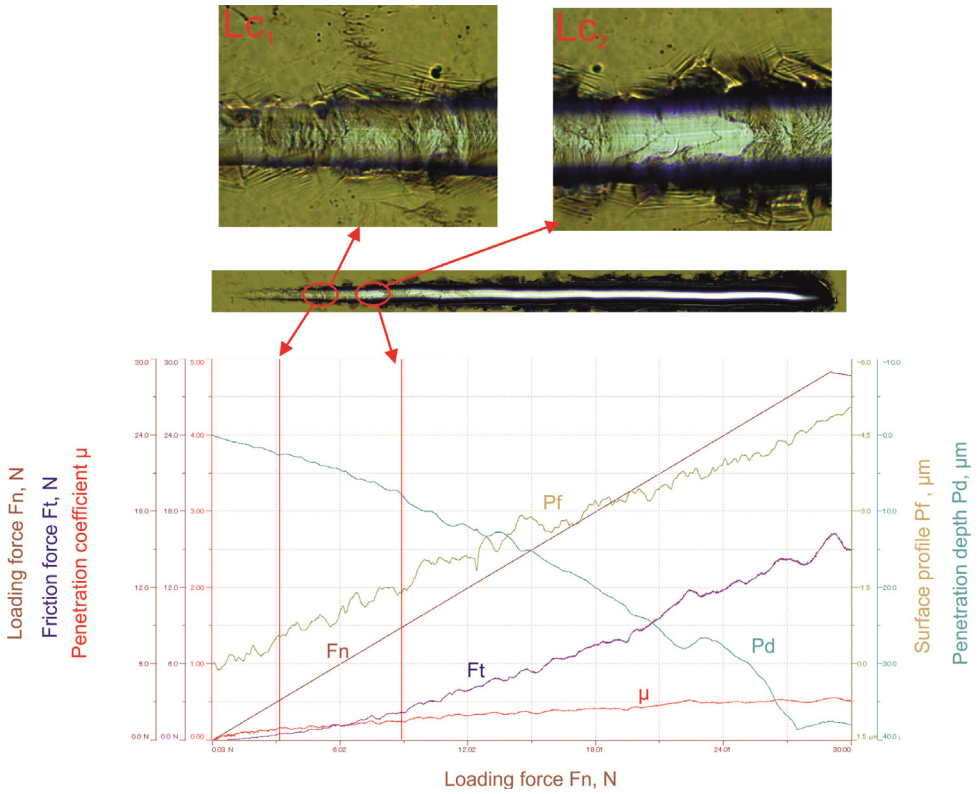

Fig. 11 – Examples of adhesion in 316LVM steel sample with ALD deposited TiO_2 film at T = 300 °C (Ft – friction force, Fn – loading force, Pf – surface profile, Pd – penetration depth, μ – penetration coefficient).

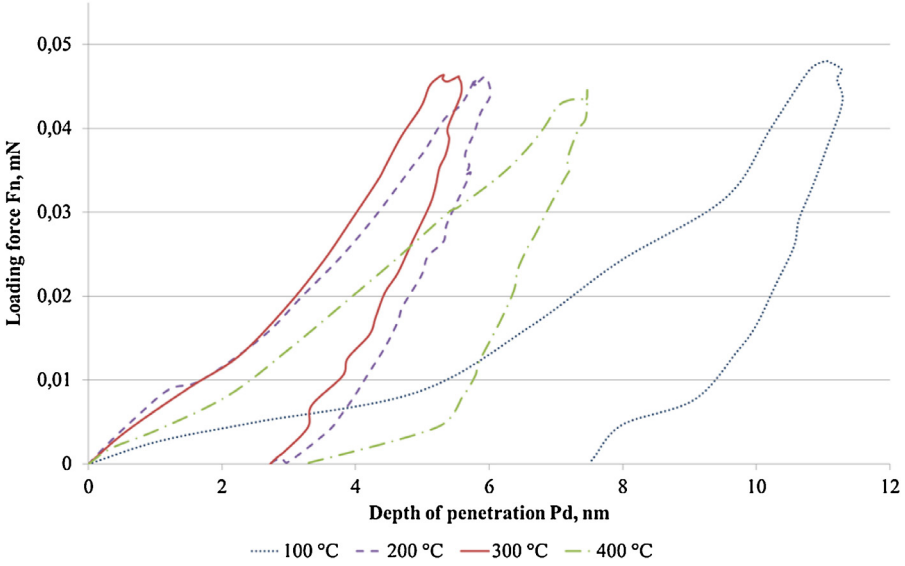

Fig. 12 – Relation between hardness of the evaluated layers and the penetration depth.

that the binding energy between the coating and the base was too low. In all cases, plastic non-continuous perforation of the layer was observed. Sobczyk-Guzenda et al. [27] investigated TiO_2 layer deposition on 316LVM steel base, making use of RF-PECVD method. The results pointed to the critical force of Lc = 30 mN, effecting in delamination. Sidane et al. [28] evaluated adhesion of HAP – TiO_2 layers, grown by sol–gel method, to the base of 316LVM steel. They observed that in such case the value of the critical force was Lc = 6430 mN. The grown layers, both TiO_2 jak and HAP-TiO_2, showed remarkably lower adhesion to 316LVM steel base than that observed in the variant proposed by the authors. Similar studies were carried out by Walke et al. [29], who applied the sol–gel method to deposit SiO_2 on 316LVM steel used to manufacture the blood-contacting implants. The value of the critical force which resulted in complete destruction of the layer was close to the evaluated case and equaled Lc_2 = 7700 mN.

3.6.2. *Nanohardness test*

Results of the measurements are included in Table 6 and Fig. 12. The values observed pointed to different hardness of the layers, depending on the applied deposition temperature. The highest hardness was noted for the layers grown at T = 200 °C and T = 300 °C, where the value was respectively H_{IT} = 10,666 MPa (T = 200 °C) and H_{IT} = 11,058 MPa (T = 300 °C). Sobczyk-Guzenda et al. [27] investigated nanohardness of TiO_2 film grown on 316LVM steel with the use of RF-PECVD and sol–gel methods. The hardness achieved was respectively H_{IT} = 4600 MPa (for RF-PECVD) and H_{IT} = 4900 MPa (for sol–gel). Compared to the literature [30–32], the TiO_2 layers grown with the use of ALD show significantly higher hardness.

Table 6 – Hardness of TiO_2 film on 316LVM steel.

Temperature of the ALD process	Nanohardness H_{IT}, MPa	
	Average	Standard deviation
100 °C	4071	±816
200 °C	10,666	±805
300 °C	11,058	±588
400 °C	7744	±935

4. Conclusions

The study evaluated the effect of temperature of TiO_2 deposition with ALD method, on 316LVM steel base, used to manufacture, e.g. the vascular stents. ALD temperature has a major role in the final quality of the surface layer grown with the use of such method, regardless of the type of the base. Practically, the temperatures applied range between 100 °C and 400 °C. Therefore, the authors evaluated the electrochemical and mechanical properties of the layers grown within this temperature range, aiming for the most favourable variant of surface modification. The investigations carried out showed that the process temperature has an effect upon the ultimate quality of the surface layer. It was observed that the increase of temperature had an adverse influence on corrosive resistance in the artificial plasma and contributed to formation of a double (porous) layer showing decreased tightness, as proved by EIS tests. This is why the number of metallic ions marked after 28-day exposure was highest at the temperature of 400 °C, as proved by ICP-AES investigations. Further on, assessment of the coating adhesion to the base showed that too low process temperature T = 100 °C had an adverse effect on mechanical properties, resulting in substantially reduced critical force Lc. Moreover, it was observed that the layers grown at temperatures T = 100 °C and 400 °C showed significantly lower hardness than those grown at T = 200 °C and

300 °C. The same tendency was noted in case of adhesion. Adhesion of coatings grown over the implants' surfaces contributes remarkably to their usability, while delamination may result in a local voltaic cell, initiating therefore the corrosive process which effect in reduces haemocompatibility of a device. On the other hand, the performed surface wettability tests showed no influence of ALD temperature in the obtained angle values. It was observed however that the values were favourably increased as compared to uncoated samples. All surface layers were hydrophobic which is an advantage in case of such medical devices. To sum up, the tests carried out within the framework of this study proved explicitly that the most advantageous pattern of electrochemical and mechanical properties, in the artificial plasma environment, was shown by the TiO_2 film deposited with the use of ALD method at the temperature $T = 200$ °C. Further blood-contact cytotoxicity and biocompatibility tests shall be designed to provide comprehensive evaluation of performance of such layers.

Acknowledgements

The project was funded by the National Science Centre allocated on the basis of the decision No. 2014/13/D/ST8/03230.

REFERENCES

[1] B.D. Ratner, A.S. Hoffman, F.J. Schoen, J.E. Lemons, Biomaterials Science. An Introduction to Materials in Medicine, Elsevier Academic Press, Amsterdam, Oxford, New York, Tokyo, 2004, pp. 137–152.
[2] M. Fedel, Blood compatibility of diamond-like carbon (DLC) coatings, Diamond-Based Materials for Biomedical Applications (2013) 71–102.
[3] T. Hanava, In vivo metallic biomaterials and surface modification, Materials Science Engineering 267 (1999) 2360–2366.
[4] M. Basiaga, R. Jendruś, W. Walke, Z. Paszenda, M. Kaczmarek, M. Popczyk, Influence of surface modification on properties of stainless steel used for implants, Archives of Metallurgy and Materials 60 (4) (2015) 2965–2969.
[5] D. Siva, R. Krishna, Y. Sun, Thermally oxidised rutile-TiO_2 coating on stainless steel for tribological properties and corrosion resistance enhancement, Applied Surface Science 252 (2005) 1107–1121.
[6] G.X. Shen, Y.C. Chen, L. Lin, C.J. Lin, D. Scantlebury, Study on a hydrophobic nano-TiO_2 coating and its properties for corrosion protection of metals, Electrochimica Acta 50 (2005) 5083–5089.
[7] A. Karambakhsh, A. Afshar, P. Malekinejad, Corrosion resistance and color properties of anodized Ti-6Al-4V, Journal of Materials Engineering and Performance 21 (2012) 121–127.
[8] B. Díaza, J. Swiatowska, V. Mauricea, A. Seyeux, B. Normand, E. Härkönen, M. Ritala, P. Marcus, Electrochemical and time-of-flight secondary ion mass spectrometry analysis of ultra-thin metal oxide (Al_2O_3 and Ta_2O_5) coatings deposited by atomic layer deposition on stainless steel, Electrochimica Acta 56 (2011) 10516–10523.
[9] B.S. Lim, A. Rahtu, R.G. Gordon, Atomic layer deposition of transition metals, Nature Materials 2 (2003) 749–754.
[10] L. Aarik, T. Arroval, R. Rammula, H. Mändar, V. Sammelselg, J. Aarik, Atomic layer deposition of TiO_2 from $TiCl_4$ and O_3, Thin Solid Films 542 (2013) 100–107.
[11] M. Basiaga, M. Staszuk, W. Walke, Z. Opilski, Mechanical properties of ALD TiO_2 layers on stainless steel substrate, Materialwissenschaft & Werkstofftechnik 47 (5) (2016) 1–9.
[12] H. Kumagai, Y. Masuda, T. Shinagawa, Self-limiting nature in atomic-layer epitaxy of rutile thin films from $TiCl_4$ and H_2O on sapphire (001) substrates, Journal of Crystal Growth 314 (2011) 146–150.
[13] M.R. Saleem, P. Silfsten, S. Honkanen, J. Turunen, Thermal properties of TiO_2 films grown by atomic layer deposition, Thin Solid Films 520 (2012) 5442–5446.
[14] Standard: ASTM F2129 – Electrochemical Corrosion Testing of Surgical Implants (Standard Test Method for Conducting Cyclic Potentiodynamic Polarization).
[15] ISO 10993-15 Biological Evaluation of Medical Devices – Part 15: Identification and Quantification of Degradation Products from Metals and Alloys.
[16] PN-EN 1071-3:2007. Advanced Technical Ceramics. Methods of Test for Ceramic Coatings. Part 3. Determination of Adhesion and Other Mechanical Failure Modes in an Attempt to Scratch.
[17] PN-EN ISO 14577-1 Metallic Materials-Instrumented Indentation Test for Hardness Materials Parameters – Part 1: Test Method.
[18] A. Kajzer, W. Kajzer, J. Dzielicki, D. Matejczyk, The study of physicochemical properties of stabilizing plates removed from the body after treatment of pectus excavatum, Acta of Bioengineering and Biomechanics 2 (2015) 35–44.
[19] A. Kajzer, W. Kajzer, K. Gołombek, M. Knol, J. Dzielicki, W. Walke, Corrosion resistance, EIS and wettability of the implants made of 316LVM steel used in chest deformation treatment, Archives of Metallurgy and Materials 61 (2) (2016) 3283–3298.
[20] E. Marin, L. Guzman, A. Lanzutti, W. Ensinger, L. Fedrizzi, Multilayer Al_2O_3/TiO_2 atomic layer deposition coatings for the corrosion protection of stainless steel, Thin Solid Films 522 (2012) 283–288.
[21] M. Leskeläa, M. Kemella, K. Kuklia, V. Porea, E. Santalaa, M. Ritalaa, J. Lub, Exploitation of atomic layer deposition for nanostructured materials, Materials Science and Engineering C 27 (5-8) (2007) 1504–1508.
[22] C.X. Shan, X. Hou, K.-L. Choy, Corrosion resistance or TiO_2 films grown on stainless steel by atomic layer deposition, Surface & Coatings Technology 202 (2008) 2399–2402.
[23] J. Aarik, A. Aidla, H. Maèndar, V. Sammelselg, Anomalous effect of temperature on atomic layer deposition of titanium dioxide, Journal of Crystal Growth 220 (2000) 531–537.
[24] M. Catauroa, F. Bollinoa, F. Papalea, R. Giovanardib, P. Veronesib, Corrosion behavior and mechanical properties of bioactive sol-gel coatings on titanium implants, Materials Science and Engineering C 43 (2014) 375–382.
[25] L.C. Xu, Effect of surface wettability and contact time on protein adhesion to biomaterial surfaces, Biomaterials 28 (2007) 3273–3283.
[26] M. Kawashitaa, Y. Tanakab, S. Uenob, G. Liua, Z. Lic, T. Miyazakid, In vitro apatite formation and drug loading/release of porous TiO_2 microspheres prepared by sol–gel processing with different SiO_2 nanoparticle contents, Materials Science and Engineering C 50 (2015) 317–323.
[27] A. Sobczyk-Guzenda, B. Pietrzyk, W. Jakubowski, H. Szymanowski, W. Szymanski, J. Kowalski, K. Olesko, M. Gazicki-Lipman, Mechanical, photocatalytic and microbiological properties of titanium dioxide thin films synthesized with the sol–gel and low temperature plasma deposition techniques, Materials Research Bulletin 48 (2013) 4022–4031.

[28] D. Sidane, D. Chicot, S. Yala, S. Ziani, H. Khireddine, A. Iost, X. Decoopman, Study of the mechanical behavior and corrosion resistance of hydroxyapatite sol–gel thin coatings on 316 L stainless steel pre-coated with titania film, Thin Solid Films 593 (2015) 71–80.

[29] W. Walke, Z. Paszenda, M. Basiaga, P. Karasiński, M. Kaczmarek, EIS study of SiO_2 oxide film on 316L stainless steel for cardiac implants, Information Technologies in Biomedicine. Advances in Intelligent Systems and Computing, vol. 284, Springer, 2014, pp. 403–410.

[30] M. Basiaga, Z. Paszenda, W. Walke, P. Karasiński, J. Marciniak, Electrochemical impedance spectroscopy and corrosion resistance of SiO_2 coated cpTi and Ti-6Al-7Nb alloy, Information Technologies in Biomedicine. Advances in Intelligent Systems and Computing, vol. 284, Springer, 2014, pp. 411–420.

[31] M. Talha, C. Behera, O.P. Sinha, A review on nickel-free nitrogen containing austenitic stainless steels for biomedical applications, Materials Science and Engineering C 33 (7) (2013) 3563–3575.

[32] A. Zieliński, S. Sobieszczyk, T. Seramak, W. Serbiński, B. Świeczko-Żurek, A. Ossowska, Biocompatibility and bioactivity of load-bearing metallic implants, Advances in Materials Science 10 (4) (2010) 21–31.